Uncertainty propagation in criticality measures for driver assistance

Jan Erik Stellet[1], Jan Schumacher[1], Wolfgang Branz[1], J. Marius Zöllner[2]

***Abstract*— Active safety systems employ surround environment perception in order to detect critical driving situations. Assessing the threat level, e.g. the risk of an imminent collision, is usually based on criticality measures which are calculated from the sensor measurements. However, these metrics are subject to uncertainty. Probabilistic modelling of the uncertainty allows for more informed decision making and the derivation of sensor requirements.**

This work derives closed-form expressions for probability distributions of criticality measures under both state estimation and prediction uncertainty. The analysis is founded on uncertainty propagation in non-linear motion models. Finding the distribution of model-based criticality metrics is then performed using closed-form expressions for the collision probability and error propagation in implicit functions. All results are illustrated and verified in Monte-Carlo simulations.

I. Introduction

A. Motivation

Automotive collision avoidance systems are often based on criticality measures for decision making. The objective is to detect impending collisions and assess the associated risk level, i.e. the remaining driver actions in order to avoid an accident. Therefore, it is intended to quantify how a situation separates itself from safe, normal driving. Commonly used criticality measures include the *time to collision* [1], its generalisation to 2-D [2], the *time to react* [3], or the *Brake-Threat-Number (BTN)* and *Steer-Threat-Number (STN)* [4]. If a collision is unavoidable, an autonomous system intervention, e.g. automatic emergency brake, is performed.

False activations of such an intervention are clearly not acceptable. However, because the criticality measures are based on an inaccurate and incomplete environment perception, uncertainty in the current and predicted situation understanding is inevitable. Modelling these uncertainties is therefore crucial both during the system design stage, i.e. for the derivation of minimum required sensor performance, as well as for on-line decision making. Analytical models are especially important for the latter application but also provide valuable insights for the system development.

B. Related work

Collision risk metrics usually differentiate between the risk assessment for a predicted collision and the special case where no imminent collision is predicted. Thus, uncertainty propagation in criticality measures is related to the fundamental problem of collision probability estimation.

One major challenge when calculating the probability of a collision is that multivariate probability density functions (pdf) have to be integrated over the uncertain future paths of ego vehicle and object. Thus, Monte-Carlo methods have been proposed in [5]–[9]. Another approach [10] is to reformulate a collision event using a scalar distance function.

Analytical solutions on the other hand are shown in [11]–[13]. In these works, predicted trajectories are either assumed certain or the process noise is taken into account using recursive calculations for discrete-time models.

In order to evaluate the influence of sensor noise on criticality measures, Monte-Carlo simulations have been employed in [14]–[16]. Propagation of measurement noise in the *time to collision* measure is further performed with Monte-Carlo methods in [10] and the Unscented Transformation in [17]. Taking both measurement and process noise into account, probabilistic decision making with Monte-Carlo stochastic integration is proposed in [18], [19].

An example of a rigorous analytical propagation is [12] where closed-form exact and approximate distributions of the *time to collision* under measurement noise are presented. However, an analytical solution under both measurement and prediction uncertainty has not yet been discussed. Instead of modelling distributions of criticality measures, [20] examines the worst-case performance of an intervention decision strategy under bounded measurement and prediction errors.

C. Organisation of the paper

In order to structure the problem, a typical signal processing chain of an Advanced Driver Assistance System is presented in Sec. II. Subsequently, theoretical background on kinematic vehicle motion models and uncertainty propagation in these systems is discussed. The main results are derived in Sec. III. An efficient calculation of collision probabilities and novel analytical error propagation in criticality measures are introduced. Simulation results in Sec. IV illustrate these findings on the example two common risk metrics. All results are summarised in Sec. V.

II. Theoretical Background

A. Overview

The system design assumed in this work is shown in Fig. 1. Following the perception layer, a state estimator, e.g. a Kalman filter, is assumed for providing a Gaussian estimate of the relative dynamic state $\mathbf{x} \sim \mathcal{N}(\hat{\mathbf{x}}, \mathbf{\Sigma_x})$. The kinematic state vector consists of position and velocity and is denoted as $\mathbf{x} := \begin{bmatrix} x & y & v_x & v_y \end{bmatrix}^\top$. Based on these estimates, model-based criticality assessment comprises the two steps of prediction and risk assessment.

[1]Jan Erik Stellet, Jan Schumacher and Wolfgang Branz are with Robert Bosch GmbH, Corporate Research, Vehicle Safety and Assistance Systems, 71272 Renningen, Germany

[2]J. Marius Zöllner is with Research Center for Information Technology (FZI), 76131 Karlsruhe, Germany

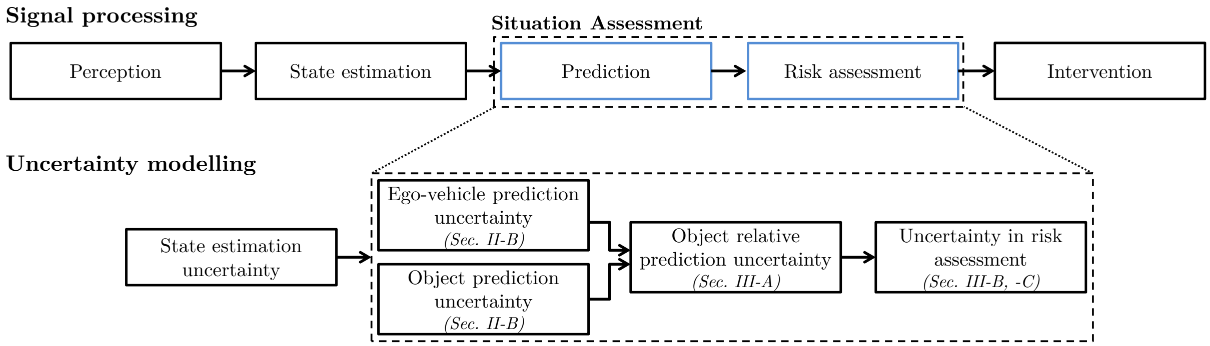

Fig. 1. Signal processing chain and outline of uncertainty modelling approach.

In this work, a ground-fixed Cartesian coordinate system and a Cartesian coordinate system which moves with the ego vehicle are used. The absolute state variables corresponding to ego vehicle or object are denoted as $\mathbf{x}^{\mathrm{E}}$ and $\mathbf{x}^{\mathrm{O}}$ respectively. Whereas $\mathbf{x}$ corresponds to the object state as seen from the ego vehicle.

B. Uncertainty propagation in kinematic motion models

At first, the foundations on uncertainty propagation in non-linear dynamic systems are reviewed. Subsequently, these are applied to two exemplary motion models used in this work.

Given an initial state estimate $\mathbf{x}(0) \sim \mathcal{N}(\hat{\mathbf{x}}(0), \boldsymbol{\Sigma}_{\mathbf{x}}(0))$, the goal is to predict its distribution at a future time instance T where the prediction model is given as a system of n non-linear, stochastic differential equations:

$$\dot{\mathbf{x}}(t) = \mathbf{f}(\mathbf{x}(t)) + \mathbf{L}\mathbf{w}(t) \ . \tag{1}$$

Here, stochastic deviations from an ideal deterministic prediction are modelled as additive white Gaussian process noise $\mathbf{w}(t) \in \mathbb{R}^{n_S}$ with time-invariant power spectral density $\mathbb{E}\left[\mathbf{w}(t)\,\mathbf{w}(t')^\top\right] = \mathbf{S}\delta(t-t')$ and $\mathbf{L} \in \mathbb{R}^{n \times n_S}$.

A Gaussian estimate $\mathcal{N}(\hat{\mathbf{x}}(T), \boldsymbol{\Sigma}_{\mathbf{x}}(T))$ of the predicted state can be derived by linearisation. For non-linear systems, this is a first-order approximation of the non-Gaussian density [21]. A more accurate propagation is achieved, e.g. with a Gaussian mixture model [22]. The Jacobian of $\mathbf{f}(\mathbf{x}(t))$ at $\mathbf{x}(t)$ is denoted as $\mathbf{F}(t) := \nabla_{\mathbf{x}(t)}\mathbf{f}(\mathbf{x}(t))$. Then, the following covariance propagation is obtained [23]:

$$\hat{\mathbf{x}}(T) = \boldsymbol{\Phi}(T,0)\,\hat{\mathbf{x}}(0)\,, \tag{2a}$$

$$\boldsymbol{\Sigma}_{\mathbf{x}}(T) = \boldsymbol{\Phi}(T,0)\,\boldsymbol{\Sigma}_{\mathbf{x}}(0)\,\boldsymbol{\Phi}^\top(T,0) + \mathbf{Q}(T,0)\,, \tag{2b}$$

$$\text{with } \mathbf{Q}(t,t_0) = \int_{t_0}^{t} \boldsymbol{\Phi}(t,\tau)\,\mathbf{L}\mathbf{S}\mathbf{L}^\top\boldsymbol{\Phi}^\top(t,\tau)\,\mathrm{d}\tau, \tag{2c}$$

$$\boldsymbol{\Phi}(t,t_0) = \exp\left(\int_{t_0}^{t}\mathbf{F}(\tau)\,\mathrm{d}\tau\right) \ . \tag{2d}$$

It may be impossible to find closed-form expressions for the transition matrix $\boldsymbol{\Phi}(t,t_0)$ in general. Fortunately, some of the most commonly used motion models in ADAS, such as the linear Constant Velocity (CV) or Constant Acceleration (CA) as well as the non-linear Constant Turn Rate and Acceleration (CTRA) models make remarkable exceptions.

1) Constant Velocity: The model describes a purely translational, non-accelerated motion in x and y direction. This simplified view is useful when an object is tracked without explicit knowledge of its orientation. The process noise $\mathbf{w}(t)$ is defined by its spectral density $\mathbf{S} = \mathrm{diag}\left(\begin{bmatrix} S_x & S_y \end{bmatrix}\right)$:

$$\begin{bmatrix} \dot{x}(t) \\ \dot{y}(t) \\ \dot{v}_x(t) \\ \dot{v}_y(t) \end{bmatrix} = \begin{bmatrix} 0 & 0 & 1 & 0 \\ 0 & 0 & 0 & 1 \\ 0 & 0 & 0 & 0 \\ 0 & 0 & 0 & 0 \end{bmatrix} \begin{bmatrix} x(t) \\ y(t) \\ v_x(t) \\ v_y(t) \end{bmatrix} + \begin{bmatrix} 0 & 0 \\ 0 & 0 \\ 1 & 0 \\ 0 & 1 \end{bmatrix} \begin{bmatrix} w_x(t) \\ w_y(t) \end{bmatrix} . \tag{3}$$

It is easily shown that $\boldsymbol{\Phi}(t,t_0) = \mathbf{I}_{4\times4} + \mathbf{F}(t-t_0)$ and thus a closed-form solution to (2) is obtained with

$$\mathbf{Q}(T,0) = \begin{bmatrix} \frac{1}{3}T^3S_x & 0 & \frac{1}{2}T^2S_x & 0 \\ 0 & \frac{1}{3}T^3S_y & 0 & \frac{1}{2}T^2S_y \\ \frac{1}{2}T^2S_x & 0 & TS_x & 0 \\ 0 & \frac{1}{2}T^2S_y & 0 & TS_y \end{bmatrix} . \tag{4}$$

2) Constant Turn Rate and Acceleration: A curvilinear trajectory is modelled by taking into account rotational and translational motion with constant acceleration a and yaw rate ω. The differential equations with process noise strength $\mathbf{S} = \mathrm{diag}\left(\begin{bmatrix} S_a & S_\omega \end{bmatrix}\right)$ are given as:

$$\begin{bmatrix} \dot{x}(t) \\ \dot{y}(t) \\ \dot{v}(t) \\ \dot{\theta}(t) \\ \dot{a}(t) \\ \dot{\omega}(t) \end{bmatrix} = \begin{bmatrix} v(t)\cos(\theta(t)) \\ v(t)\sin(\theta(t)) \\ a(t) \\ \omega(t) \\ 0 \\ 0 \end{bmatrix} + \begin{bmatrix} 0 & 0 \\ 0 & 0 \\ 0 & 0 \\ 0 & 0 \\ 1 & 0 \\ 0 & 1 \end{bmatrix} \begin{bmatrix} w_a(t) \\ w_\omega(t) \end{bmatrix} . \tag{5}$$

Here, velocity and acceleration are conveniently modelled in polar coordinates. This state vector $\mathbf{x}_{\mathrm{p}}$ is converted to Cartesian coordinates $\mathbf{x}$ using the transformation $\boldsymbol{\pi}_{\mathrm{p}}^{\mathrm{c}}(\cdot)$:

$$\boldsymbol{\pi}_{\mathrm{p}}^{\mathrm{c}}(\mathbf{x}_{\mathrm{p}}) := \begin{bmatrix} x & y & v\cos(\theta) & v\sin(\theta) \end{bmatrix}^\top . \tag{6}$$

Despite its non-linearity, (2) can be analytically solved for the CTRA model [24]. This is because $\mathbf{F}(t)$ is a strict upper diagonal matrix, which also holds for its integral. Thus, a closed-form solution for $\boldsymbol{\Phi}(t,t_0) = \mathbf{I}_{6\times6} + \int_{t_0}^{t}\mathbf{F}(\tau)\,\mathrm{d}\tau$ and finally the state covariance $\boldsymbol{\Sigma}_{\mathbf{x}}^{\mathrm{p}}(T)$ can be obtained.

In order to obtain the covariance for the state with Cartesian velocity v_x, v_y, the Jacobian $\nabla_{\mathbf{x}_{\mathrm{p}}}\boldsymbol{\pi}_{\mathrm{p}}^{\mathrm{c}}(\mathbf{x})$ of (6) is calculated. Then, $\mathbf{\Sigma_x}(T) = \left(\nabla_{\mathbf{x}_\mathrm{p}} \boldsymbol{\pi}_\mathrm{p}^\mathrm{c}\right) \cdot \mathbf{\Sigma}_\mathbf{x}^\mathrm{p}(T) \cdot \left(\nabla_{\mathbf{x}_\mathrm{p}} \boldsymbol{\pi}_\mathrm{p}^\mathrm{c}\right)^\top$ yields the final result.

Note that the uncertainty propagation (2) can be evaluated for arbitrary continuous time T. An alternative approach is pursued in [5], [8], where the prediction step of an Extended Kalman Filter is iteratively calculated for a discrete-time version of the motion model. Therefore, only a recursive solution at the discrete time steps is available.

A concluding remark on the chosen uncertainty model in (1): While human drivers can predict and assess situations based on a multitude of cues (e.g., road layout, context, interaction), current threat assessment algorithms employ range information only. When additional high-level semantic information is available, one could extend the unimodal process noise $\mathbf{w}(t)$ to a situation-dependent multimodal distribution, in order to represent alternative manoeuvres (e.g. driving straight or turning). Overall, this will narrow the likely trajectories and thus lead to higher certainty in the risk assessment.

Nevertheless, one has to be cautious about the level of rationalism that is assumed in the prediction. In fact, critical situations are often caused by a lack of mutual awareness and interaction between traffic participants [9]. Hence, it is assumed that ego vehicle and object are statistically independent in this work.

Because manoeuvre changes are not taken into consideration here, the validity of the model is certainly restricted to a short prediction horizon only. This is however not a severe limitation, as we consider situations with a high risk of an imminent collision and hence predictions for up to approximately 3 s only. It is the scope of future works to investigate the model's validity based on empirical data.

III. Uncertainty in Criticality Measures

At first, uncertainty transformation to relative coordinates, which are used in the criticality assessment, is discussed in Sec. III-A. Then, a method to derive the probability distribution $p_\kappa(\kappa)$ of a criticality measure κ from measurement and prediction uncertainty is presented in Sec. III-B and III-C. Finally, a concluding summary is given in Sec. III-D.

A. State prediction uncertainty for relative motion

In the previous section, uncertainty propagation has been considered for motion models in a common ground-fixed coordinate system. For the application of tracking and situation interpretation it is however beneficial to describe an object's motion in Cartesian coordinates which are centred and aligned to the ego vehicle's pose. These relative coordinates arise naturally when sensory information measured from the moving ego vehicle is processed.

Generally, transforming from absolute to relative coordinates is performed by a linear transformation:

$$\mathbf{x} := \mathbf{M}\left(\mathbf{x}^\mathrm{E}\right)\left(\mathbf{x}^\mathrm{O} - \mathbf{x}^\mathrm{E}\right) . \tag{7}$$

If $\mathbf{x}$ comprises Cartesian position and velocity, θ^E denotes the heading of the ego vehicle and $\mathbf{R}\left(\theta^\mathrm{E}\right)$ is a rotation matrix, then $\mathbf{M}\left(\mathbf{x}^\mathrm{E}\right)$ is defined as [25]:

$$\mathbf{M}\left(\theta^\mathrm{E}, \omega^\mathrm{E}\right) = \begin{bmatrix} \mathbf{R}\left(\theta^\mathrm{E}\right) & \mathbf{0} \\ \dot{\mathbf{R}}\left(\theta^\mathrm{E}, \omega^\mathrm{E}\right) & \mathbf{R}\left(\theta^\mathrm{E}\right) \end{bmatrix} . \tag{8}$$

However, attempting to propagate uncertainty directly in these relative coordinates poses two challenges:

1) Depending on the two involved motion models, finding the differential equations of the relative motion is difficult and potentially requires approximations [25].[1] Moreover, the challenge of calculating the uncertainty propagation as in (2) for this model remains.
2) Process noise $\mathbf{w}(t)$ is a property of the individual motion models and naturally defined in the frames of ego vehicle and object respectively. For instance, anisotropic noise is typically assumed in the longitudinal and lateral motion to account for inhomogeneous evasion capabilities. In a relative motion model, this results in a variance dependent on time-varying quantities such as the heading angle.

An approach to overcome these challenges for the design of a tracking filter is pursued in [26]: The relative object dynamic state, ego vehicle speed and yaw-rate are concatenated in an extended state vector. Thus, the process noise covariance of the extended state consists of separate block-matrices for object and ego vehicle. However, an explicit dynamic model for the relative motion is still required.

Here, it is proposed to first propagate uncertainties in absolute coordinates using (2) and then transform the resulting covariances $\mathbf{\Sigma}_\mathbf{x}^\mathrm{E}, \mathbf{\Sigma}_\mathbf{x}^\mathrm{O}$ to $\mathbf{\Sigma_x}$ in the relative frame through (7).

When $\mathbf{M}\left(\theta^\mathrm{E}, \omega^\mathrm{E}\right)$ is known without uncertainty, the propagation follows immediately:

$$\mathbf{\Sigma_x} = \mathbf{M}\left(\theta^\mathrm{E}, \omega^\mathrm{E}\right) \cdot \left(\mathbf{\Sigma}_\mathbf{x}^\mathrm{O} + \mathbf{\Sigma}_\mathbf{x}^\mathrm{E}\right) \cdot \mathbf{M}^\top\left(\theta^\mathrm{E}, \omega^\mathrm{E}\right) . \tag{9}$$

In practice, rotating by an uncertain heading angle θ^E and yaw rate ω^E introduces additional errors. Modelling the variance in the components of $\mathbf{x}$ can be pursued by rewriting (7) row-wise as a quadratic form.

To this end, the i-th row $\mathbf{m}_i^\top$ of $\mathbf{M}\left(\theta^\mathrm{E}, \omega^\mathrm{E}\right)$ is firstly rewritten as a linear mapping $\mathbf{m}_i = \tilde{\mathbf{A}}_i \mathbf{q}\left(\theta^\mathrm{E}, \omega^\mathrm{E}\right)$, where $\tilde{\mathbf{A}}_i := \nabla_\mathbf{q} \mathbf{m}_i$ and $\mathbf{q}\left(\theta^\mathrm{E}, \omega^\mathrm{E}\right)$ are the trigonometric expressions which (8) consists of. Moreover, the abbreviations $\boldsymbol{\xi} := \mathbf{x}^\mathrm{O} - \mathbf{x}^\mathrm{E}$ and $\mathbf{\Sigma}_{\boldsymbol{\xi}} := \mathbf{\Sigma}_\mathbf{x}^\mathrm{O} + \mathbf{\Sigma}_\mathbf{x}^\mathrm{E}$ are introduced. Hence:

$$x_i = \frac{1}{2} \underbrace{\begin{bmatrix} \boldsymbol{\xi}^\top & \mathbf{q}^\top\left(\theta^\mathrm{E}, \omega^\mathrm{E}\right) \end{bmatrix}}_{=:\mathbf{y}^\top} \underbrace{\begin{bmatrix} \mathbf{0}_{4\times4} & \tilde{\mathbf{A}}_i \\ \tilde{\mathbf{A}}_i^\top & \mathbf{0}_{4\times4} \end{bmatrix}}_{=:\mathbf{A}_i} \underbrace{\begin{bmatrix} \boldsymbol{\xi} \\ \mathbf{q}\left(\theta^\mathrm{E}, \omega^\mathrm{E}\right) \end{bmatrix}}_{=:\mathbf{y}} .$$

Then, results on moments of quadratic forms provide [27]:

$$\begin{aligned} \Sigma_{\mathbf{x},ij} &= \mathrm{cov}\left(\mathbf{y}^\top \mathbf{A}_i \mathbf{y}, \mathbf{y}^\top \mathbf{A}_j \mathbf{y}\right) \\ &= \mathrm{tr}\left(\mathbf{\Sigma}_{\mathbf{m}_i,\mathbf{m}_j} \mathbf{\Sigma}_{\boldsymbol{\xi}}\right) + \boldsymbol{\xi}^\top \mathbf{\Sigma}_{\mathbf{m}_i,\mathbf{m}_j} \boldsymbol{\xi} + \mathbf{m}_i^\top \mathbf{\Sigma}_{\boldsymbol{\xi}} \mathbf{m}_j , \\ \mathbf{\Sigma}_{\mathbf{m}_i,\mathbf{m}_j} &= \mathrm{cov}\left(\mathbf{m}_i, \mathbf{m}_j\right) = \nabla_{\boldsymbol{\theta}} \mathbf{m}_i \mathbf{\Sigma}_{\boldsymbol{\theta}} \left(\nabla_{\boldsymbol{\theta}} \mathbf{m}_j\right)^\top , \\ \boldsymbol{\theta} &:= \begin{bmatrix} \theta^\mathrm{E} & \omega^\mathrm{E} \end{bmatrix}^\top . \end{aligned} \tag{10}$$

[1] In tracking applications, the exact influence of the ego vehicle's rotation is often approximated in the form of pseudo acceleration inputs [25].

B. Probability of a collision

The risk assessment measures considered in this work are defined conditionally that a collision is predicted to take place if no further action is taken. It is the objective of these risk metrics κ to quantify the remaining evasive actions or reaction time left. If no collision is predicted, e.g., either because two vehicles are driving on different lanes or their relative velocity is positive, the criticality metric is set to a boundary value which defines a least critical situation.[2]

In order to model the uncertainty in a criticality measure, the probability of taking on a boundary value is analysed first. Therefore, the collision probability over a future trajectory needs to be calculated given an uncertainty model for the predicted trajectory from Sec. III-A.

At a point in time τ where the predictions are given as the joint probability density $p_{\mathbf{x}^{\mathrm{E}},\mathbf{x}^{\mathrm{O}}}\left(\mathbf{x}^{\mathrm{E}}(\tau),\mathbf{x}^{\mathrm{O}}(\tau)\right)$, the instantaneous probability of a collision event $C_{(\tau)}$ is [6]

$$\mathrm{P}\left(C_{(\tau)}\right)=\int_{\mathbf{x}^{\mathrm{O}}}\int_{\mathbf{x}^{\mathrm{E}}} I_{\mathrm{C}}\left(\mathbf{x}^{\mathrm{E}},\mathbf{x}^{\mathrm{O}}\right) p_{\mathbf{x}^{\mathrm{E}},\mathbf{x}^{\mathrm{O}}}\left(\mathbf{x}^{\mathrm{E}},\mathbf{x}^{\mathrm{O}}\right)\mathrm{d}\mathbf{x}^{\mathrm{E}}\mathrm{d}\mathbf{x}^{\mathrm{O}} \tag{11}$$

where $I_{\mathrm{C}}\left(\mathbf{x}^{\mathrm{E}},\mathbf{x}^{\mathrm{O}}\right)$ denotes a collision indicator function which is based on the object geometries $\mathcal{S}\left(\mathbf{x}^{E}\right)$, $\mathcal{S}\left(\mathbf{x}^{E}\right)$:

$$I_{\mathrm{C}}\left(\mathbf{x}^{\mathrm{E}},\mathbf{x}^{\mathrm{O}}\right)=\begin{cases}1 & \mathcal{S}\left(\mathbf{x}^{\mathrm{E}}\right)\cap\mathcal{S}\left(\mathbf{x}^{\mathrm{O}}\right)\neq\emptyset\\ 0 & \mathcal{S}\left(\mathbf{x}^{\mathrm{E}}\right)\cap\mathcal{S}\left(\mathbf{x}^{\mathrm{O}}\right)=\emptyset\end{cases} . \tag{12}$$

The complexity of this problem is due to:

- It is required to integrate multivariate probability functions over the two contours.
- Only a single time instant is considered in (11). Thus, a statement on the overall collision probability $\mathrm{P}\left(C_{(0,T)}\right)$ within a time interval $t\in[0,T]$ is further to be derived.

Monte-Carlo approaches are presented in [5]–[10] with different means taken to reduce the computational burden. For example, the assumption of independent states and combination of both contours to a single integration volume in relative coordinates can be leveraged [7].

Analytical expressions for Gaussian state distributions are derived in [8], [11], [12]. In [8], the evolution of the instantaneous probability of a collision over time is interpreted as a criticality measure. It is suggested in [11] to remove the time-dependence by calculating the maximum value over all time steps. A rigorous probabilistic derivation is presented in [12]. Here, the motion is separated in longitudinal and lateral direction. Moreover, simple rectangular shapes are assumed in car following scenarios where the heading angle is neglected. This structures the problem to determine the probability distributions of

1) the point in time ttc *(time to collision)* where both vehicles share the same longitudinal position x and
2) the relative lateral distance y at this time instant in comparison to a critical corridor of width w.

In a first step, the distribution $p_{ttc}(t)$ is determined. For correlated Gaussian errors in the relative longitudinal dynamics $x(0), v_x(0)$, the exact distribution and a Gaussian approximation are derived in [12]. The latter one will be extended in the following Sec. III-C to further account for uncertain trajectories.

Secondly, the probability of a collision within the time interval $t\in[0,T]$ is determined from the distribution of the relative lateral position $y(\tau)$ conditional on $\tau=ttc$. In the case of independent motion in x and y, this reads [12]:

$$\mathrm{P}\left(C_{(0,T)}\right)=\int_0^T\int_{-w/2}^{w/2} p_y\left(y(\tau)\,|\tau\right)p_{ttc}(\tau)\,\mathrm{d}\tau\mathrm{d}y\ . \tag{13}$$

A simplification is proposed here by neglecting the uncertainty of ttc and replacing $p_{ttc}(t)$ with a dirac function:

$$p_{ttc}(\tau)=\delta\left(\tau-\mu_{ttc}\right)\ . \tag{14}$$

The reasoning is that the time-dependent $p_y(y(\tau))$ can be approximated by its average distribution $p_y(y(\mu_{ttc}))$ as long as $p_{ttc}(\tau)$ is reasonably narrow. Certainly, correlation between longitudinal and lateral motion would also affect this assumption. This simplifies (13) to:

$$\mathrm{P}\left(C_{(0,T)}\right)=\int_{-w/2}^{w/2} p_y\left(y\left(\mu_{ttc}\right)\right)\mathrm{d}y\ . \tag{15}$$

Therefore, instead of numerically integrating a non-Gaussian probability density in (13), it is only required to evaluate the cumulative distribution function of a normal distribution in (15), e.g. with a lookup table.

C. Propagation from uncertain state predictions to criticality

Having addressed the probability of a collision, this section studies the uncertainty in commonly used risk metrics.

1) Problem formulation: Risk metrics are based on the current estimate of the (relative) motion state $\mathbf{x}(0)$ and the objective is to distinguish critical from normal driving situations. These metrics κ are usually designed as scalar functions $\psi(\cdot)$:

$$\kappa=\psi\left(\mathbf{x}(0)\right)\ . \tag{16}$$

Decision making on a system intervention can then be based on one or multiple [3] thresholds.

Uncertainty in κ is obviously induced by errors in the estimated $\mathbf{x}(0)$. The variance Σ_κ can be analytically quantified via Gaussian error propagation, i.e. linearisation of $\psi(\cdot)$:

$$\Sigma_\kappa=\left(\nabla_{\mathbf{x}(0)}\psi\left(\mathbf{x}(0)\right)\right)\cdot\mathbf{\Sigma}_{\mathbf{x}}(0)\cdot\left(\nabla_{\mathbf{x}(0)}\psi\left(\mathbf{x}(0)\right)\right)^\top\ . \tag{17}$$

However, a second source of uncertainty are deviations between the true future evolution of a situation and the prediction which is implicitly assumed in $\psi(\cdot)$. A novel methodology for Gaussian error propagation with consideration of prediction uncertainty is proposed in the following.

2) Methodology: Firstly, an equivalent formulation of the criticality measure (16) as an implicit function of the predicted state $\mathbf{x}(T)$ is introduced. Secondly, a result on error propagation in implicit functions [28] is used. Finally, the results from Sec. III-A on uncertainty in the prediction $\mathbf{x}(T)$ are inserted which yields the propagation to Σ_κ.

[2]Without loss of generality, this boundary value is chosen as $\kappa=0$ here.

As a first step towards the reformulated criticality, the (linear) state prediction model is abbreviated as $\lambda(\mathbf{x}(0), u, t)$:

$$\lambda(\mathbf{x}(0), u, t) := \mathbf{x}(t) = \mathbf{\Phi}(t, 0)\,\mathbf{x}(0) + \mathbf{b}u \,. \tag{18}$$

Here, u denotes an (optional) system input, for example a deceleration applied by the driver. As has been explained in [11], a model-based criticality measure can now be defined as condition on a function $\boldsymbol{\phi}(\cdot)$ of the predicted state $\mathbf{x}(T)$:

$$\boldsymbol{\phi}(\mathbf{x}(T)) = \mathbf{0} \,. \tag{19}$$

An explicit criticality measure $\kappa = \psi(\mathbf{x}(0))$ is then derived by inserting the model (18) and solving for the combination $\boldsymbol{\alpha} = \begin{bmatrix} T & u \end{bmatrix}^\top$ of prediction time and the required input in order to fulfil the condition (19):

$$\boldsymbol{\alpha} := \begin{bmatrix} T \\ \kappa \end{bmatrix} = \mathrm{sol}_{(t,u)}\left\{\boldsymbol{\phi}(\mathbf{x}(t)) = \mathbf{0}\right\} \tag{20}$$

$$= \mathrm{sol}_{(t,u)}\left\{\boldsymbol{\phi}(\lambda(\mathbf{x}(0), u, t)) = \mathbf{0}\right\} \,. \tag{21}$$

For instance, one may define the condition that a collision is just avoided by a braking deceleration u. That is, at time T where the first contact with the object ($x(T) = 0$) occurs, the relative velocity should vanish ($v_x(T) = 0$). Solving for u gives the minimum required deceleration.

Thanks to this implicit definition it is possible to calculate the variation of the solution $\boldsymbol{\alpha} := \begin{bmatrix} T & \kappa \end{bmatrix}^\top$ when $\mathbf{x}(T)$ is varied. That is, both uncertainty on the estimate of $\mathbf{x}(0)$ as well as in the prediction model can be taken into account. The covariance matrix $\mathbf{\Sigma}_{\boldsymbol{\alpha}}$ follows by first-order error propagation and the lower right element contains $\mathrm{Var}(\kappa)$:

$$\mathbf{\Sigma}_{\boldsymbol{\alpha}} = \begin{bmatrix} \Sigma_T & \Sigma_{T\kappa} \\ \Sigma_{\kappa T} & \Sigma_\kappa \end{bmatrix} = \left(\nabla_{\mathbf{x}(T)}\boldsymbol{\alpha}\right) \cdot \mathbf{\Sigma}_{\mathbf{x}}(T) \cdot \left(\nabla_{\mathbf{x}(T)}\boldsymbol{\alpha}\right)^\top . \tag{22}$$

In order to find the required gradient $\nabla_{\mathbf{x}(T)}\boldsymbol{\alpha}$ of (20) the implicit function theorem can be used [28]:

$$\nabla_{\mathbf{x}(T)}\boldsymbol{\alpha} = -\left[\nabla_{(t,u)}\boldsymbol{\phi}(\lambda(\mathbf{x}(0), u, t))\right]^{-1} \nabla_{\mathbf{x}(T)}\boldsymbol{\phi}(\mathbf{x}(T)) \,. \tag{23}$$

Finally, we are now in a position to insert result (10) on the prediction uncertainty $\mathbf{\Sigma}_{\mathbf{x}}(T)$ into (22). In the following, this general result will be illustrated for two criticality measures.

3) Time to collision: A particularly simple metric, which forms the basis for more advanced time-based metrics, such as the *time to react* [3], is the *time to collision* ttc:

$$ttc = -\frac{x(0)}{v_x(0)} \,. \tag{24}$$

This measure is based on the CV[3] motion model (3):

$$\lambda(\mathbf{x}(0), t) = \mathbf{x}(t) = \begin{bmatrix} \mathbf{I}_{2\times2} & t\mathbf{I}_{2\times2} \\ \mathbf{0}_{2\times2} & \mathbf{I}_{2\times2} \end{bmatrix} \mathbf{x}(0) \,. \tag{25}$$

A one-dimensional condition on the predicted state $\phi(\mathbf{x}(T))$ defines a collision event in longitudinal direction:

$$ttc = \mathrm{sol}_{(t)}\left\{\begin{bmatrix} 1 & 0 & 0 & 0 \end{bmatrix} \cdot \mathbf{x}(t) = 0\right\} \,. \tag{26}$$

[3]A more sophisticated form based on a Constant Acceleration model is given in [11]. On the one hand, incorporating a more precise model with higher moments of the motion reduces the prediction uncertainty. On the other hand, it is required to estimate additional dynamic quantities.

The gradient is calculated according to (23):

$$\nabla_{\mathbf{x}(T)} ttc = -\left[\frac{\mathrm{d}}{\mathrm{d}t}\left(x(0) + v_x(0)\,t\right)\right]^{-1} \cdot \nabla_{\mathbf{x}} x$$
$$= -\begin{bmatrix} \frac{1}{v_x(0)} & 0 & 0 & 0 \end{bmatrix} \,. \tag{27}$$

Now, an assumption on the predicted state uncertainty $\mathbf{\Sigma}_{\mathbf{x}}(T)$ has to be made. Basically, the method is not limited to a specific approach. As it has been argued, treating ego vehicle and object separately first can lead to better models.

A special case is to consider the same prediction model $\lambda(\mathbf{x}(0), t)$ as employed in the derivation of the criticality measure. Inserting the predicted covariance $\mathbf{\Sigma}_{\mathbf{x}}(T)$ for the linear CV model as derived in Sec. II-B yields an interesting result in closed form:

$$\Sigma_{ttc} = \left(\nabla_{\mathbf{x}(T)} ttc\right) \cdot \mathbf{\Sigma}_{\mathbf{x}}(T) \cdot \left(\nabla_{\mathbf{x}(T)} ttc\right)^\top \tag{28}$$
$$= \left(\nabla_{\mathbf{x}(0)} ttc\right) \cdot \mathbf{\Sigma}_{\mathbf{x}}(0) \cdot \left(\nabla_{\mathbf{x}(0)} ttc\right)^\top - \frac{x^3(0)}{3v_x^5(0)} S_x$$

Here, $\nabla_{\mathbf{x}(0)} ttc$ denotes the gradient of (24) with respect to $\mathbf{x}(0)$. Therefore, the classical error propagation result (17) is recovered with an additional term that accounts for the prediction uncertainty.

4) Brake Threat Number: While the *time to collision* is a popular and easily interpretable measure, it is only implicitly related to a driver's capabilities to avoid a collision.

A second group of criticality measures assesses the required future driver inputs to avoid a collision. These have a clear physical interpretation, e.g. deceleration or yaw rate. Usually, the physical quantities are normalised (e.g. to the maximum possible value each) which yields comparable criticality measures for different evasive actions.

Here, the basic interpretation of the *required longitudinal acceleration* a_{req}, which is also known as *Brake Threat Number (BTN)* [4], [11] after normalisation, will be analysed:

$$a_{\mathrm{req}} = -\frac{v_x^2(0)}{2x(0)} \,. \tag{29}$$

For the motion dynamics, a CV model with longitudinal ego-vehicle acceleration input a is assumed:

$$\lambda(\mathbf{x}(0), a, t) = \mathbf{x}(t) = \begin{bmatrix} \mathbf{I}_{2\times2} & t\mathbf{I}_{2\times2} \\ \mathbf{0}_{2\times2} & \mathbf{I}_{2\times2} \end{bmatrix} \mathbf{x}(0) - \mathbf{b}a \,,$$
$$\mathbf{b} = \begin{bmatrix} 1/2t^2 & 0 & t & 0 \end{bmatrix}^\top \,. \tag{30}$$

Condition (19) on the final state is defined as $x(T) = 0$, $v_x(T) = 0$ and thus [11]:

$$\begin{bmatrix} T \\ a_{\mathrm{req}} \end{bmatrix} = \mathrm{sol}_{(t,a)}\left\{\begin{bmatrix} 1 & 0 & 0 & 0 \\ 0 & 0 & 1 & 0 \end{bmatrix} \cdot \mathbf{x}(t) = \mathbf{0}\right\} \,. \tag{31}$$

Solving (31) with (30) yields a_{req} as in (29) and $T = -2x(0)/v_x(0)$. Note that the prediction time is twice the ttc here which increases the influence of the process noise.

The gradient (23) evaluated at the expected values is:

$$\nabla_{\mathbf{x}(T)} a_{\mathrm{req}} = \begin{bmatrix} \frac{v_x^2(0)}{2x(0)} & 0 & 0 & 0 \end{bmatrix} \,. \tag{32}$$

Employing $\boldsymbol{\Sigma}_{\mathbf{x}}(T)$ for the CV model (30) yields the following closed-form result:

$$\Sigma_{a_{\mathrm{req}}} = \left(\nabla_{\mathbf{x}(0)} a_{\mathrm{req}}\right) \cdot \boldsymbol{\Sigma}_{\mathbf{x}}(0) \cdot \left(\nabla_{\mathbf{x}(0)} a_{\mathrm{req}}\right)^{\top} - \frac{2 v_x(0)}{3 x(0)} S_x . \tag{33}$$

Here, the first term is the classical error propagation (17).

D. Summary of main results

This section provided the main theoretical contributions on uncertainty propagation in criticality measures. As criticality metrics are usually defined as functions of relative dynamic states, a rigorous analysis of error propagation in relative dynamics is performed in Sec. III-A. The idea is to separately model the process noise of ego vehicle and object first and propagate the uncertainty from absolute to relative motion.

Uncertainty propagation in the criticality measure κ is split in two aspects presented in Sec. III-B and Sec. III-C. At first, the probability $1 - \mathrm{P}\left(C_{(0,T)}\right)$ of taking on a boundary value which corresponds to the no collision case is analysed. Secondly, the distribution $\mathcal{N}\left(\mu_\kappa, \Sigma_\kappa\right)$ of the risk metric conditional on a predicted collision event is modelled. Here, a novel method to analytically account for uncertain prediction models with Gaussian process noise is introduced.

In conclusion, the criticality measure is distributed as a mixture of two components:

$$p_\kappa(\kappa) = \left(1 - \mathrm{P}\left(C_{(0,T)}\right)\right) \cdot \delta(\kappa) + \mathrm{P}\left(C_{(0,T)}\right) \cdot \mathcal{N}\left(\mu_\kappa, \Sigma_\kappa\right) . \tag{34}$$

IV. Simulation

The focus of this work is on how state estimation and prediction uncertainties propagate to criticality measures. In the following, Monte-Carlo simulations are used to verify the analytic results, given an assumed model of these uncertainties. Validating statistical models for specific sensor (e.g. stereo vision [29]) and prediction errors is thus out of this work's scope.

A. Setup and parameter values

All simulations are based on the configuration shown in Fig. 2. The ego vehicle is moving in x-direction with constant velocity according to the CTRA model (5), towards an object which is crossing into the driving corridor (CV model (3)). Using an environment sensor the object state is measured and the distribution of two criticality measures evaluated. Initial values and the process noise parameters are given in table I.

B. Uncertainty in predicted states

At first, $N_{\mathrm{sample}} = 100$ trajectory predictions of the ego vehicle and object are calculated. The analytical propagation (2) is solved using the respective models and shown in form of 90% confidence ellipses. Evaluated at six different time steps, the results in Fig. 3(a) show good correspondence.

Secondly, the resulting relative trajectories as seen from the ego vehicle are visualised in Fig. 3(b). The propagation model from Sec. III-A is shown with (10) and without (9) considering the uncertainty in the rotation angle. Neglecting the heading errors leads to too narrow confidence ellipses, most notable at far distances. In these cases, even small angle errors lead to high lateral deviations.

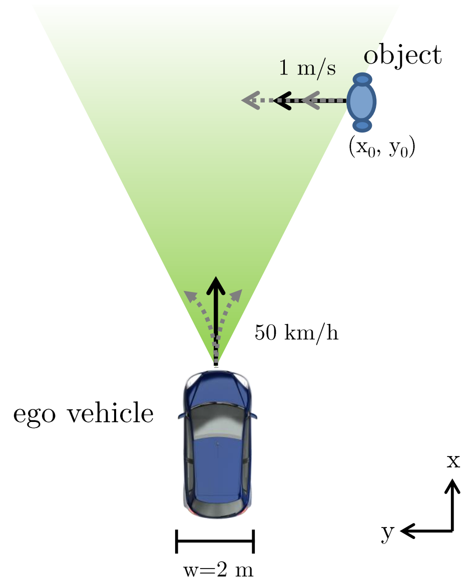

Fig. 2. Illustration of the simulation setup.

TABLE I
SIMULATION PARAMETERS

Variable	Value
Ego vehicle: Initial state	$\mathbf{x}^{\mathrm{E}}(0)$: $x(0) = 0,\ y(0) = 0,\ v(0) = 13.89\,\mathrm{m/s},\ \theta(0) = 0,\ a(0) = 0,\ \omega(0) = 0$
Initial uncertainty	$\boldsymbol{\Sigma}_{\mathbf{x}}^{\mathrm{E}}(0) = \mathbf{0}_{6\times 6}$
Process noise	$S_a^{\mathrm{E}} = \left(0.31\,\mathrm{m/s^3}\right)^2 \mathrm{s}^{-1}$, $S_\omega^{\mathrm{E}} = \left(1.28\,°/\mathrm{s}^2\right)^2 \mathrm{s}^{-1}$
Object: Initial state	$\mathbf{x}^{\mathrm{O}}(0)$: $x(0) = 80\,\mathrm{m},\ y(0) = -5.75\,\mathrm{m},\ v_x(0) = 0,\ v_y(0) = 1\,\mathrm{m/s}$
Initial uncertainty	$\boldsymbol{\Sigma}_{\mathbf{x}}^{\mathrm{O}}(0) = \mathrm{diag}\left[0.5\,\mathrm{m}\ 0.5\,\mathrm{m}\ 0.2\,\mathrm{m/s}\ 0.2\,\mathrm{m/s}\right]^2$
Process noise	$S_x^{\mathrm{O}} = S_y^{\mathrm{O}} = \left(0.5\,\mathrm{m/s^2}\right)^2 \mathrm{s}^{-1}$
Critical corridor	$w = 2\,\mathrm{m}$
Normalisation	$BTN = \frac{a_{\mathrm{req}}}{-6\,\mathrm{m/s^2}}$

C. Probability of a collision

Simulated trajectories are now repeatedly calculated starting from different time steps t_0. That is, the prediction is started from the mean values $\mathbf{x}^{\mathrm{E}}(t_0)$, $\mathbf{x}^{\mathrm{O}}(t_0)$ with uncertainties $\boldsymbol{\Sigma}_{\mathbf{x}}(t_0) = \boldsymbol{\Sigma}_{\mathbf{x}}(0)$.[4] Collision probabilities over the relative distance $x(t_0)$ are shown in (4). Smaller distances mean less time and therefore less chances for evasive actions which results in a higher collision probability.

Three models are compared to the Monte-Carlo results: Firstly, the complex model (13) by [12] is numerically evaluated. Here, the Gaussian propagation with process noise uncertainty from (28) is inserted for the required density

[4] Assuming a constant initial uncertainty on $\mathbf{x}(t_0)$ does not account for the typical behaviour of a tracking filter where the estimates improve over time. This time-dependence of $\boldsymbol{\Sigma}_{\mathbf{x}}(t_0)$ is neglected here for clarity.

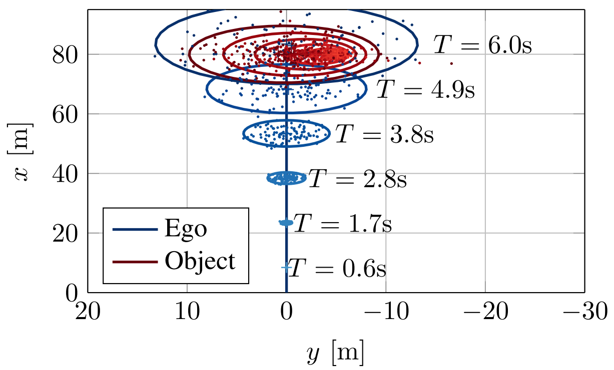

(a) Absolute positions. The uncertainty propagation (2) is calculated for the CTRA model (5) (ego vehicle) and the CV model (3) (object).

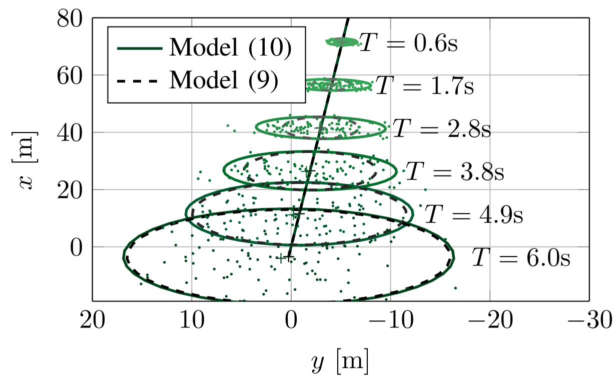

(b) Relative positions. Modelled uncertainty ellipses are calculated with and without considering the uncertainty in heading θ^{E} and yaw rate ω^{E}.

Fig. 3. Uncertainty in predicted position: Monte-Carlo simulation results ($N_{\text{sample}} = 10^2$ iterations) and analytical model (uncertainty ellipses corresponding to the 90%-environment).

$p_{ttc}(t)$ of the time to collision. Secondly, the simplified model (15) which does not consider uncertainty in the longitudinal direction is shown and almost identical results are achieved.

Finally, the original model from [12] is calculated where a non-Gaussian distribution for $p_{ttc}(t)$ is employed in (13) but process noise is not taken into account. Much higher collision probabilities are obtained because trajectories are falsely assumed certain. Especially for high initial distances, i.e. long prediction times, the process noise influence is clearly visible over the state estimation uncertainty.

D. Uncertainty in criticality measures

Similar to the previous section, trajectories are now simulated from three different times t_0 on. For each trajectory, the true values of two criticality measures are evaluated: The true ttc (24) follows from the simulated time step where ego vehicle and object collide for the first time. Ground truth values for the normalised *required longitudinal acceleration* from (29) are calculated from the true relative velocity at the time of collision. Hence, the true a_{req} is given as the true velocity difference divided by twice the true ttc.

The distributions (normalised frequency and empirical CDF) of these criticality measures are shown in Fig. 5. For

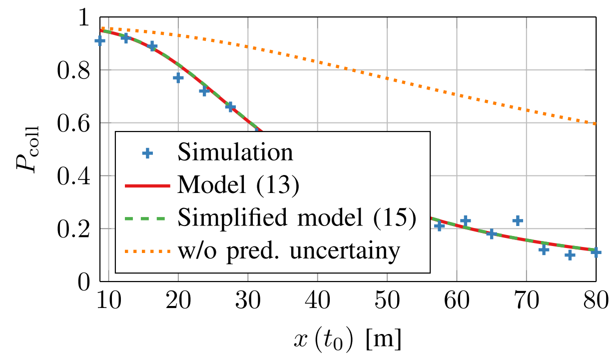

Fig. 4. Collision probability over initial position $x(0)$. Monte-Carlo simulation results ($N_{\text{sample}} = 10^4$ iterations) are compared to the model (13) by [12] extended with prediction uncertainty and the simplified expression from (15). For comparison, the original model [12] which only considers uncertainty in the estimated initial values is shown.

comparison, the models obtained in Sec. III-C are visualised and a high correspondence is achieved.

In order to quantitatively evaluate the goodness of fit, the Kolmogorov-Smirnov statistic is calculated. This metric is defined as the maximum difference between two CDFs. At first, a non-parametric reference distribution is sampled from $N_{\text{ref}} = 10^5$ iterations. A naïve sampling approach ($N_{\text{sample}} = 10^2 \ldots 10^4$) is performed for comparison to the analytical model. The deviations are then calculated between the cumulative distribution of the reference on the one hand and the distributions of the analytical model or the sampling approach on the other hand.

The results reveal that it requires approximately $N_{\text{sample}} = 10^4$ iterations in order to yield the same accuracy as the analytical approach. Although there are certainly more sophisticated approaches for efficient sampling, e.g. [5], [6], these promising results encourage further extensions.

V. Conclusion

This paper has addressed uncertainty modelling for criticality assessment in driver assistance systems. First, an analytical method for collision probability calculation from [12] is extended to state estimation and prediction uncertainties. Moreover, a simplified approximation has been proposed and evaluated in Monte-Carlo simulations.

Secondly, a method for analytical uncertainty propagation in criticality measures under consideration of measurement and process noise is introduced. The solution is evaluated in simulations of two criticality measures. Furthermore, the number of iterations in a naïve numerical sampling approach is analysed that is required to achieve a comparably accurate distribution model as the analytical result.

Given that the current work [9] proposes to generalise classical criticality measures to probabilistic metrics, the analytical results could prove very useful to determine closed-form expressions. A second possible extension of this contribution is to consider multi-modal state predictions in order to describe different manoeuvres.

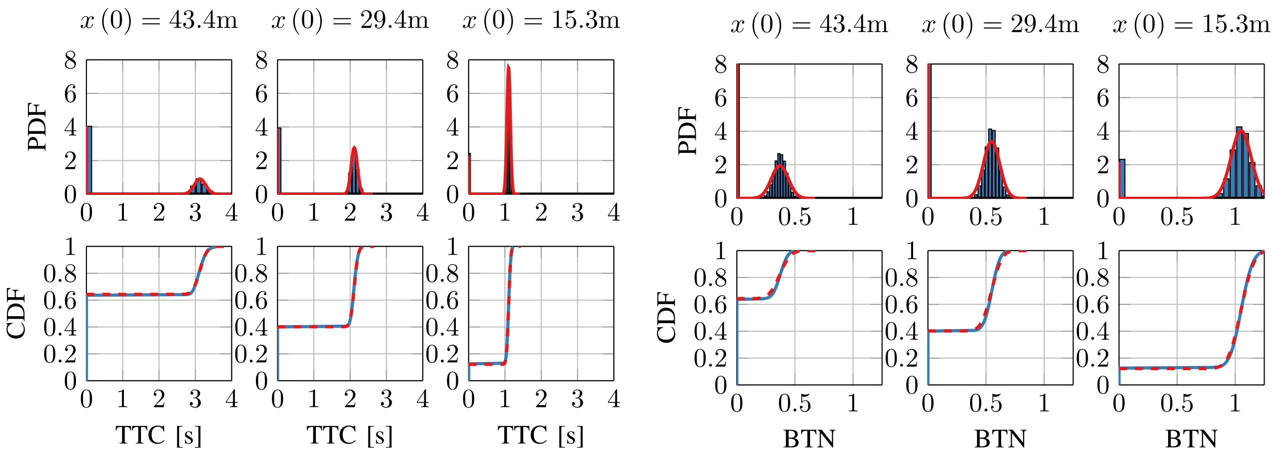

(a) Uncertainty in *time to collision*.

(b) Uncertainty in normalised *required longitudinal acceleration*.

Fig. 5. Uncertainty model (red) for criticality measures compared to simulated error distribution (blue). $N_{\text{sample}} = 10^5$ trajectories have been sampled for each initial position. Analysing each trajectory for the occurrence of a collision leads to the sample distribution of the criticality measures. The model (34) matches the simulated results. Higher initial distances lead to longer prediction times T and therefore a lower collision probability $\mathrm{P}\left(C_{(0,T)}\right)$. This causes higher peaks at the boundary value $\kappa = 0$.

References

[1] R. Labayrade, C. Royere, and D. Aubert, "Experimental assessment of the rescue collision-mitigation system," *Vehicular Technology, IEEE Transactions on*, vol. 56, no. 1, pp. 89–102, 2007.

[2] J. Ward, G. Agamennoni, S. Worrall, and E. Nebot, "Vehicle collision probability calculation for general traffic scenarios under uncertainty," in *Intelligent Vehicles Symposium Proceedings, IEEE*, pp. 986–992, 2014.

[3] J. Hillenbrand and K. Kroschel, "A study on the performance of uncooperative collision mitigation systems at intersection-like traffic situations," in *Cybernetics and Intelligent Systems, 2006 IEEE Conference on*, pp. 1–6, June 2006.

[4] G. Engelman, J. Ekmark, L. Tellis, N. Tarabishy, G. Joh, R. Trombley, and R. Williams, "Threat level identification and quantifying system," 2006. US Patent.

[5] A. Lambert, D. Gruyer, G. Pierre, and A. Ndjeng, "Collision probability assessment for speed control," in *Intelligent Transportation Systems (ITSC), 11th International IEEE Conference on*, pp. 1043–1048, 2008.

[6] N. Du Toit and J. Burdick, "Probabilistic collision checking with chance constraints," *Robotics, IEEE Transactions on*, vol. 27, no. 4, pp. 809–815, 2011.

[7] C. Braeuchle, J. Ruenz, F. Flehmig, W. Rosenstiel, and T. Kropf, "Situation analysis and decision making for active pedestrian protection using Bayesian networks," in *6. Tagung Fahrerassistenzsysteme*, 2013.

[8] A. Houenou, P. Bonnifait, and V. Cherfaoui, "Risk assessment for collision avoidance systems," in *Intelligent Transportation Systems (ITSC), 17th International IEEE Conference on*, pp. 386 – 391, 2014.

[9] M. Schreier, V. Willert, and J. Adamy, "Bayesian, maneuver-based, long-term trajectory prediction and criticality assessment for driver assistance systems," in *Intelligent Transportation Systems (ITSC), 17th International IEEE Conference on*, pp. 334–341, 2014.

[10] A. Berthelot, A. Tamke, T. Dang, and G. Breuel, "Handling uncertainties in criticality assessment," in *Intelligent Vehicles Symposium (IV), IEEE*, pp. 571–576, 2011.

[11] J. Jansson, *Collision Avoidance Theory : with Application to Automotive Collision Mitigation*. PhD thesis, Linköping University, Department of Electrical Engineering, 2005.

[12] P.-J. Nordlund and F. Gustafsson, "Probabilistic conflict detection for piecewise straight paths," Tech. Rep. 2871, Linköping University, Automatic Control, 2008.

[13] S. Patil, J. van den Berg, and R. Alterovitz, "Estimating probability of collision for safe motion planning under gaussian motion and sensing uncertainty," in *Robotics and Automation (ICRA), IEEE International Conference on*, pp. 3238–3244, 2012.

[14] P. Zheng and M. McDonald, "The effect of sensor errors on the performance of collision warning systems," in *Intelligent Transportation Systems (ITSC), 2003 International IEEE conference on*, pp. 469–474, 2003.

[15] J. Hillenbrand, *Fahrerassistenz zur Kollisionsvermeidung*. PhD thesis, Universität Karlsruhe, 2008.

[16] T. Dirndorfer, M. Botsch, and A. Knoll, "Model-based analysis of sensor-noise in predictive passive safety algorithms," in *Proceedings of the 22nd Enhanced Safety of Vehicles Conference*, 2011.

[17] A. Berthelot, A. Tamke, T. Dang, and G. Breuel, "A novel approach for the probabilistic computation of time-to-collision," in *Intelligent Vehicles Symposium (IV), IEEE*, pp. 1173–1178, 2012.

[18] R. Karlsson, J. Jansson, and F. Gustafsson, "Model-based statistical tracking and decision making for collision avoidance application," in *American Control Conference, Proceedings of the 2004*, vol. 4, pp. 3435–3440, 2004.

[19] M. Brännström, F. Sandblom, and L. Hammarstrand, "A probabilistic framework for decision-making in collision avoidance systems," *Intelligent Transportation Systems, IEEE Transactions on*, vol. 14, no. 2, pp. 637–648, 2013.

[20] J. Nilsson and M. Ali, "Sensitivity analysis and tuning for active safety systems," in *Intelligent Transportation Systems (ITSC), 2010 13th International IEEE Conference on*, pp. 161–167, 2010.

[21] A. W. Long, K. C. Wolfe, M. Mashner, and G. S. Chirikjian, "The banana distribution is Gaussian: A localization study with exponential coordinates.," in *Robotics: Science and Systems*, 2012.

[22] F. Havlak and M. Campbell, "Discrete and continuous, probabilistic anticipation for autonomous robots in urban environments," *Robotics, IEEE Transactions on*, vol. 30, no. 2, pp. 461–474, 2014.

[23] A. Gelb, ed., *Applied optimal estimation*. Cambridge, Mass.: M.I.T. Press, 1974.

[24] A. Kelly, "Linearized error propagation in odometry," *The International Journal of Robotics Research*, vol. 23, no. 2, pp. 179–218, 2004.

[25] R. Altendorfer, "Observable dynamics and coordinate systems for automotive target tracking," in *Intelligent Vehicles Symposium (IV), IEEE*, pp. 741–746, 2009.

[26] C. Otto, *Fusion of Data from Heterogeneous Sensors with Distributed Fields of View and Situation Evaluation for Advanced Driver Assistance Systems*. PhD thesis, Karlsruhe Institute of Technology, Karlsruhe, 2013.

[27] A. Mathai and S. Provost, *Quadratic Forms in Random Variables*. Statistics: A Series of Textbooks and Monographs, Taylor & Francis, 1992.

[28] J. C. Clarke, "Modelling uncertainty: A primer," *Tutorial of Department of Eng. Science*, 1998.

[29] H. Badino, *Binocular Ego-Motion Estimation for Automotive Applications*. PhD thesis, Goethe Universität Frankfurt am Main, 2008.